

Nonlinear analysis of the progressive collapse of reinforced concrete plane frames using a multilayered beam formulation

Análise não linear do colapso progressivo de pórticos planos de concreto armado utilizando elemento de viga com seção transversal discretizada em camadas

C. E. M. OLIVEIRA ^{a,b}
claudioernani@yahoo.com.br

E. A. P. BATELO ^a
everton.batelo@gmail.com

P. Z. BERKE ^b
pberke@ulb.ac.be

R. A. M. SILVEIRA ^a
ricardo@em.ufop.br

T. J. MASSART ^b
thmassar@ulb.ac.be

Abstract

This work investigates the response of two reinforced concrete (RC) plane frames after the loss of a column and their potential resistance for progressive collapse. Nonlinear dynamic analysis is performed using a multilayered Euler/Bernoulli beam element, including elasto-viscoplastic effects. The material nonlinearity is represented using one-dimensional constitutive laws in the material layers, while geometrical nonlinearities are incorporated within a corotational beam formulation. The frames were designed in accordance with the minimum requirements proposed by the reinforced concrete design/building codes of Europe (fib [1-2], Eurocode 2 [3]) and Brazil (NBR 6118 [4]). The load combinations considered for PC analysis follow the prescriptions of DoD [5]. The work verifies if the minimum requirements of the considered codes are sufficient for enforcing structural safety and robustness, and also points out the major differences in terms of progressive collapse potential of the corresponding designed structures.

Keywords: progressive collapse, reinforced concrete, nonlinear analysis, corotational formulation, layer discretization.

Resumo

Este trabalho investiga a resposta de dois pórticos planos de concreto armado à perda de uma coluna e sua capacidade de resistir ao colapso progressivo. A análise não linear dinâmica é realizada utilizando um elemento de viga baseado na teoria de Euler/Bernoulli com seção transversal discretizada em camadas. A não linearidade física é representada através de relações constitutivas unidimensionais, incluindo efeitos viscoplásticos. A não linearidade geométrica é incorporada através de uma formulação corrotacional. Os pórticos foram projetados de acordo com os requisitos mínimos das normas de projeto/construção de estruturas de concreto armado Europeias (fib [1-2], Eurocode 2 [3]) e Brasileiras (NBR 6118 [4]). As combinações de carregamento consideradas na análise de colapso progressivo estão de acordo com DoD [5]. O trabalho verifica se os requisitos mínimos das normas consideradas são suficientes para garantir a robustez e a segurança estrutural e aponta também as diferenças mais relevantes em termos da suscetibilidade dos pórticos ao colapso progressivo.

Palavras-chave: colapso progressivo, concreto armado, análise não linear, formulação corrotacional, discretização em camadas.

^a Department of Civil Engineering, Federal University of Ouro Preto, Ouro Preto, MG, Brazil;

^b Building, Architecture, and Town Planning Department, Université Libre de Bruxelles, Brussels, Belgium.

1. Introduction

Progressive collapse corresponds to a structural failure mechanism triggered by the irreversible damage of one or more key structural elements which forces a redistribution of the loads and internal forces in the structure (Li *et al.* [6]), resulting in changes in the loading of the transversal sections of the beams and columns. This may, in turn, initiate further propagation of structural damage by the progressive failure of the overstressed remaining structural elements.

Progressive collapse (PC) is usually described as a catastrophic dynamic behavior of civil engineering structures (Kim *et al.* [7]) that is influenced by both material (Tsai and Lin [8]; Kwasniewski [9]) and geometrical nonlinearities (Tan and Pham [10]). It leads to financial and, sometimes, human losses (Marjanishvili [11]). Many authors have investigated how to prevent progressive collapse by (1) identifying key elements of which failure may initiate PC, and (2) enhancing the overall structural robustness in order to enforce proper and adequate load redistribution to guarantee the stability of the remaining structure (Izzuddin [12]; Khandelwal and El-Tawil [13]).

Section '10.3 Estados limites últimos (ELU)' on NBR 6118 [4] specifically establishes that the safety of reinforced concrete structures must always be verified against: the limit states related to the depletion of the resistant capacity in the complete structure (and in its individual structural elements) considering, among others, the geometrically nonlinear effects; the limit states caused by dynamic solicitations and; the progressive collapse limit state.

NBR 6118 [4] also defines the appropriate flexural reinforcement for guarantying local structural ductility against progressive collapse. However, this definition is made only for flexural reinforcement of RC slabs, not beams or columns. Since no specific guidelines are given on how the verification against progressive collapse should be performed, our contribution consists in developing and applying a dedicated computational tool for the study of the structural response to extreme loading with a relatively low number of modeling assumptions. Our approach includes a dynamic description of the problem with a physically-based sectional degradation of the composite cross sections (*i.e.*, the reinforcement ratio and scheme are explicitly represented), rate-dependent material behavior of the constituents and catenary effects due to the developed geometrically nonlinear framework. Section 2 describes our contributions to the computational modeling of progressive collapse and to the numerical analysis of reinforced concrete structures.

In this work, the progressive collapse phenomenon is investigated by analyzing the structural response of two plane frames that represent a five story reinforced concrete (RC) building, designed in accordance with the European (Eurocode 2 [3]) and the Brazilian building codes (NBR 6118 [4]). Even though sharing the same architectural geometry, the obtained frames are different in terms of loads, element cross sections, reinforcement scheme, reinforcement ratio, and consequently, structural robustness, since these codes prescribe different requirements. The Eurocode-based design was carried out using the commercial software Diamonds (Buildsoft [14]) while the Brazilian design was performed on Cypecad (Cype [15]). More detailed information on these frames and their design process can be found in Section 3.

Section 4 presents the numerical tool and provides information on the multiscale approach (Iribarren *et al.* [16]) used to investigate the PC structural behavior in this work, the description of the corotational

beam formulation (Crisfield [17]; Battini [18]) and the material constitutive models. Section 5 is aimed at the presentation and the discussion of the results obtained in nonlinear dynamic analysis. Finally, conclusions and perspectives of this work are presented in Section 6.

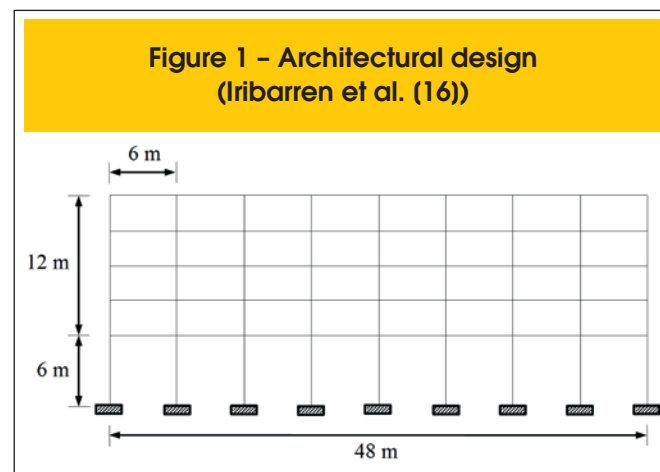
2. Main contributions

The prime numerical novelty of our approach is the introduction of catenary effects in a layered beam formulation for composite cross-sections using a corotational framework, which was not included in earlier modeling attempts (Iribarren *et al.* [16]). The extension of the numerical approach with additional complexity allows a better approximation of the physical phenomenon, since it reduces the number of modeling assumptions. This approach leads to a more realistic analysis due to the coupling of many different aspects of the structural behavior, from material properties to the interaction between the deformed geometry and the loads. The majority of works concerning the verification of progressive collapse usually considers structural designs based on European, North-American or Asian building codes. To the best knowledge of the authors, the type of progressive collapse verification performed here was not attempted before for a NBR-based building. The application of the resulting computational tool to the comparison between two structures designed following different building codes, European and Brazilian, but having identical architectural geometry is a second originality of the presented work.

3. Structural design

The plane frames consist of an 18 m high office building with five levels. The ground floor height is 6 m and the height of the other floors is 3 m each. The frame is 48 m long, equally divided in 6 m bays as shown in Figure 1. Since the presented work aims at investigating the influence of catenary effects, due to the large changes in the geometry, the removal of an interior column was considered. A similar procedure was adopted by Lew *et al.* [19], Yi *et al.*, [20].

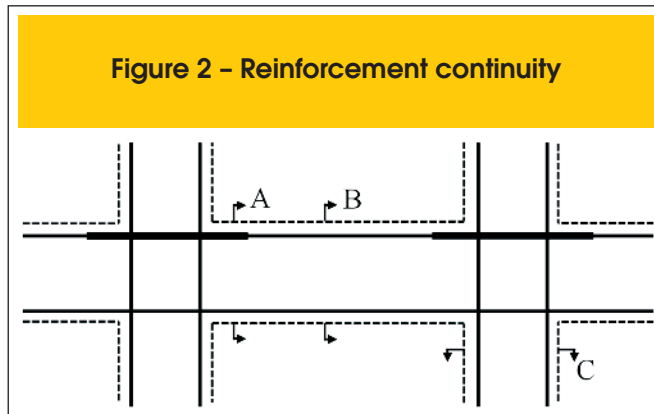
The Eurocode-based design was carried out using the commercial software Diamonds (Buildsoft [14]) and presented in Iribarren *et al.* [16], from where the parameters used in this work were directly taken. The material parameters and geometry of the structural elements



therefore assume European practical values. On the other hand, the Brazilian design was specifically performed for this work on Cypecad (Cype [15]), assuming the minimum specifications of NBR 6118 [4]. Thirty centimeters thick concrete slabs were used for the Eurocode-based frame, including a concrete cover layer of 10 cm. As discussed by Lee and Scaloni [21], Eurocode 2 [3] does not define minimum thickness for concrete slabs. Instead, the thickness is obtained as a function of the final reinforcement ratio. The European design assumes minimum reinforcement ratio (Iribarren *et al.* [16]), therefore it is correct to assume that the thickness of 20 cm used in that work is also minimum. Slabs of 13 cm are used for the Brazilian design (without any cover layer). The lack of a cover layer in the Brazilian building is justified by the herein assumed methodology of obtaining a design based on minimum requirements. These slabs do not provide any resistance; however, they were adequately dimensioned and verified against maximum allowable displacements.

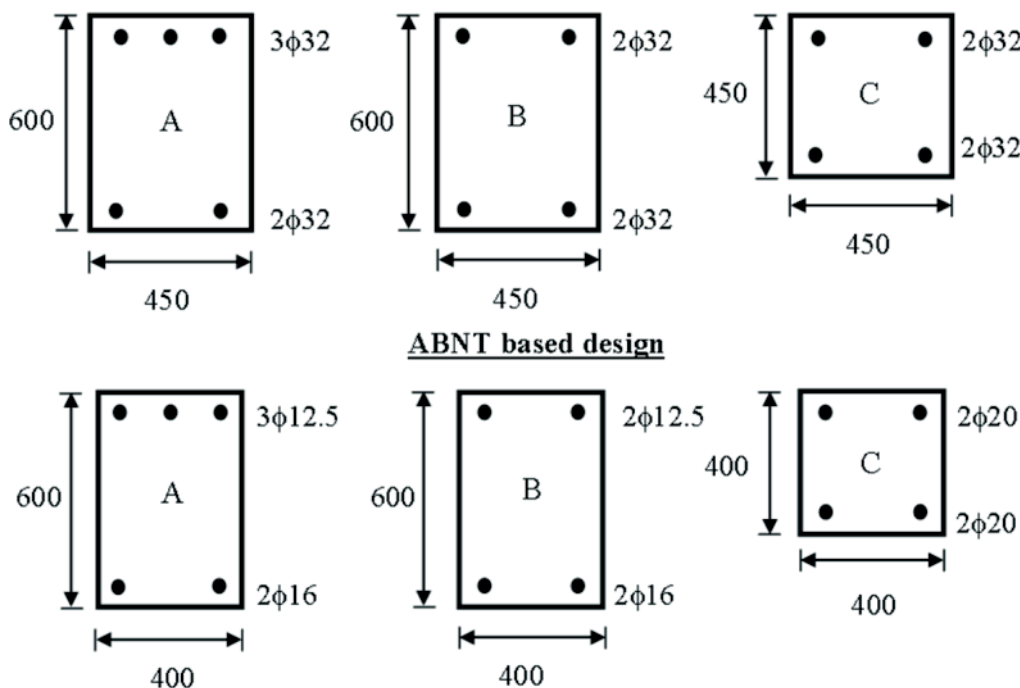
Live and dead loads are summarized in Table 1. The total load, shown in the same table, combines the total dead load value with 50% of the live loads, as recommended by DOD [5]. The self-weight load is translated into loads per unit length through the multiplication of the reinforced concrete weight density (24 kN/m³) by the volume of the structural element and subsequent division by its length. For self-weight of the slabs, the length is taken as the beam length:

- for the Eurocode-based frame:
(0.30m X 6m X 6m X 24kN/m³) /6m = 43.2kN/m
 - for the NBR-based frame:
(0.13m X 6m X 6m X 24kN/m³) /6m = 18.7kN/m
- The following assumptions were made during the design process:



- all floor beams are the same, since the same loads were considered at all floors;
- all columns are considered the same, *i.e.* although upper floor columns bear smaller loads, they have the same section and reinforcement scheme as ground columns;
- the height and the width of a structural element are constant along the length;
- assuming Aggressiveness Class II, the NBR-based design has a concrete rebar cover of 2.5 cm; a 5 cm concrete rebar cover is taken for the European design, as in Iribarren *et al.* [16];
- the bottom reinforcement is assumed continuous in both designs;
- the continuity of 2/3 of the top beam reinforcement (Figs. 2 and 3) is considered in both designs;

Figure 3 - Reinforcement schemes
(A, B and C correspond to the sections defined on Figure 2; all values in millimeters)



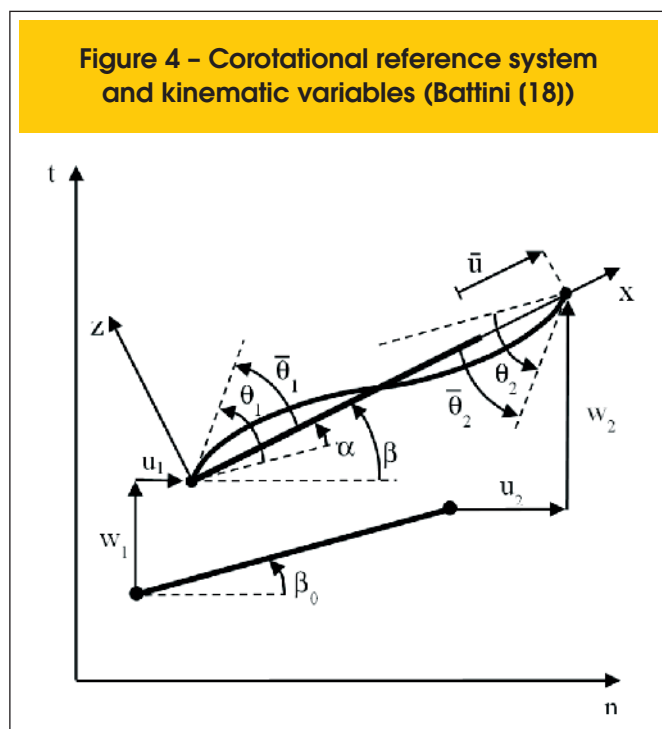
- Bond and anchorage were considered during the design process but are not included in the progressive collapse analysis;
 - Perfect bonding between concrete and steel is assumed;
 - stirrups are considered during design, but not represented in the PC analysis, *i.e.* the increase in the concrete strength and ultimate strain resulting from the confinement are not taken into account.
- Although the design of the Eurocode-based building is the same as the one presented by Iribarren *et al.* [16], the present analysis applies a further developed numerical formulation that includes nonlinear geometrical effects (catenary effects). Another difference resides in the fact that concrete strength under tension is not taken into account here, based on usual reinforced concrete practice. Besides, the influence of strain rate effects was not taken into account in Iribarren *et al.* [16] for the case middle column removal. These different features are described in the next section.

4. Geometrically nonlinear formulation with a multilayered beam approach

The main contribution of this work from a computational point of view is the incorporation of the multiscale computation of sectional stresses (Iribarren *et al.* [16]) into the geometrically nonlinear kinematics described by a corotational Bernoulli beam formulation. This section summarizes the main ingredients of the computational modeling tool. It presents the main aspects of the corotational formulation used for introducing geometrically nonlinear effects in the multiscale numerical formulation, as well as the adopted constitutive laws for the materials and the governing equations in structural dynamics.

4.1 Corotational beam kinematics

Geometrically nonlinear effects, such as catenary actions, are



effects that take place when changes in geometry have significant influence on the structural behavior (Bonet and Wood [22]). In the works by researchers as Battini *et al.* [23], Souza *et al.* [24], Lew *et al.* [19] and Yi *et al.* [20] the importance of considering these effects when analyzing steel/reinforced concrete/composite structures was clearly demonstrated. Tan and Pham [10] have also shown that catenary effects may play an important role on mitigating PC. In this work, the applied geometrically nonlinear beam kinematics represented by a corotational formulation allows for an investigation of possible catenary effects.

The corotational formulation, as presented in Crisfield [17] and Battini [18], is a reinterpretation of the deformation of a beam element or, in the most general case, a tridimensional body. This reinterpretation consists in using a local reference system attached to the beam element, different from the global, structural reference system (Fig. 4).

In this corotational approach, strains and stresses in a given element are computed in the (individual) local reference system attached to this structural element, which allows *decoupling the rigid body rotation from the actual deformation*. The relation between the displacements in the global structural reference system, $\{q_e\}^T = \{u_1, w_1, \theta_1, u_2, w_2, \theta_2\}$, and the ones in the local system of a structural element, $\{\bar{q}_e\}^T = \{\bar{u}, \bar{\theta}_1, \bar{\theta}_2\}$, is given by:

$$\begin{Bmatrix} \bar{u} \\ \bar{\theta}_1 \\ \bar{\theta}_2 \end{Bmatrix}^T = \begin{bmatrix} l_f - l_i \\ \theta_1 - \alpha \\ \theta_2 - \alpha \end{bmatrix} = \begin{bmatrix} l_f - l_i \\ \theta_1 - (\beta - \beta_0) \\ \theta_2 - (\beta - \beta_0) \end{bmatrix} \quad (1)$$

where l_f , l_i and α denote the deformed length, the undeformed length and the rigid body rotation of the element, respectively, β represents the current angle between the element and the global reference system, and β_0 represents the original value of this angle in the undeformed configuration.

In this work, a linear shape function is used for interpolating the axial displacements in the local frame of the beam element, while a cubic interpolation is used for the transverse displacements:

$$u = \frac{x}{l_i} \bar{u}$$

$$w = x \left(1 - \frac{x}{l_i}\right)^2 \bar{\theta}_1 + \frac{x^2}{l_i} \left(\frac{x}{l_i} - 1\right)^2 \bar{\theta}_2 \quad (2)$$

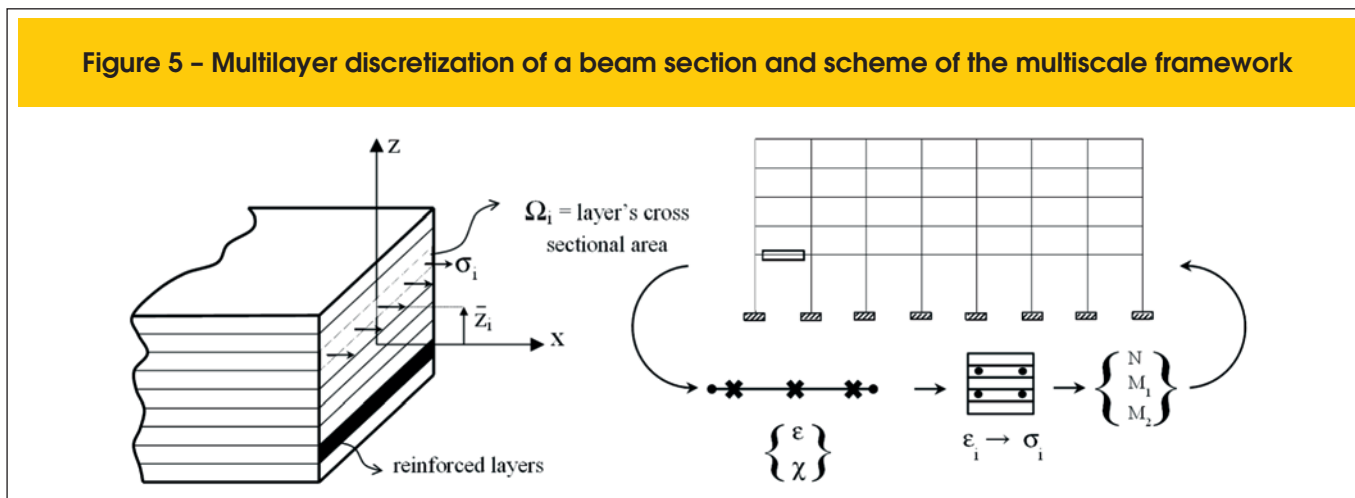
where \bar{u} , $\bar{\theta}_1$ and $\bar{\theta}_2$ are the axial elongation and the nodal rotations in the local corotational frame.

The average axial strain and beam curvature computed at an integration point of the beam finite element are therefore given by:

$$\bar{\varepsilon} = \frac{\partial u}{\partial x} = \frac{\bar{u}}{l_i}$$

$$\chi = \frac{\partial^2 w}{\partial x^2} = \left(-\frac{4}{l_i} + \frac{6}{l_i^2} x\right) \bar{\theta}_1 + \left(-\frac{2}{l_i} + \frac{6}{l_i^2} x\right) \bar{\theta}_2 \quad (3)$$

Figure 5 – Multilayer discretization of a beam section and scheme of the multiscale framework



4.2 Multilayer discretization of an Euler-Bernoulli beam

The formulation uses a layer discretization of the transversal section for determining stresses in the section of an Euler-Bernoulli beam finite element. Internal forces are obtained from the integration of sectional stresses over three Gauss points along the length of the element.

The discretization of the transversal sections, defined at the Gauss points along the length of the beam, consists of the portioning of the reinforced concrete (composite) section into longitudinal layers (Fig. 5). Note that, this produces a multilevel description that links the dynamic equilibrium on the structural level to the equilibrium of the generalized forces applied at the transversal sections.

The average axial strain and beam curvature computed at an integration point (Eq. 3) are used to obtain the total (axial) strain in each layer:

$$\epsilon_i = \bar{\epsilon} - \bar{z}_i \chi \tag{4}$$

where $\bar{\epsilon}$ is the beam axial strain and, for each layer i , \bar{z}_i is the position of layer center of mass with respect to the neutral axis of the section, χ is the beam curvature and ϵ_i is the total axial strain in a given layer. Note that Eq. (4) implies the assumption of perfect strain compatibility between the layers. This – among others – precludes the modeling of delamination between concrete and steel. Using (nonlinear) constitutive relationships for concrete and steel, it is therefore possible to determine the one-dimensional axial stresses acting in each layer, $\sigma_{i,conc.}$ and $\sigma_{i,steel}$. A mixture rule is then used for obtaining the total axial stress, as shown below:

$$\sigma_i = \frac{\Omega_i - \Omega_{i,steel}}{\Omega_i} \sigma_{i,conc.} + \frac{\Omega_{i,steel}}{\Omega_i} \sigma_{i,steel} \tag{5}$$

where σ_i is the one-dimensional total stress on layer i , Ω_i is the layer total cross-sectional area and $\Omega_{i,steel}$ is the fraction of the layer

cross-sectional area occupied by steel. Equation 5 is based on a perfect bonding assumption between concrete and steel within a given layer.

At each integration point (represented on Figure 5 by cross marks along the element), the section generalized stresses are obtained using:

$$\Sigma^{gen} = \begin{bmatrix} N \\ M \end{bmatrix} = \begin{bmatrix} \sum \sigma_i \Omega_i \\ -\sum \sigma_i \bar{y}_i \Omega_i \end{bmatrix} \tag{6}$$

These generalized stresses are used to obtain an *internal force vector*, $\{f_{int}^{local}\}^T = \{N \ M_1 \ M_2\}$, which is conjugated to the *displacement vector in the local frame* given in Eq. (1). The global (structural) internal force vector $\{f_{int}^{global}\}^T = \{f_1^n \ f_1^c \ f_2^n \ f_2^c\}$ can then be deduced from $\{f_{int}^{local}\}^T$ as shown in Crisfield [17] and Battini [18]. Detailed technical information on the derivation of these quantities and the stiffness matrix of the finite element can also be found in the latter works.

The main advantage of this approach is that it makes possible the physical representation of the reinforcement within the cross section and of a gradual sectional degradation effect, consequence of progressive layer failure.

4.3 Constitutive models for concrete and steel

The multilayered beam formulation presented uses one-dimensional constitutive laws for concrete and steel to determine the stresses in each material and, afterwards, in each layer. According to Eurocode 2 [3], class C30 concrete and S500 steel were used for the European structural design. As mentioned before, the design process of the Brazilian structure was aimed at producing a frame based on the minimum parameters of NBR 6118 [4], including the material properties as concrete strength and steel strength. C20 concrete is the lowest concrete class allowed by NBR 6118 [4] (except for reinforced concrete foundations, for which it is acceptable to use C15 concrete). For that reason concrete C20 was adopted for the Brazilian structure in association with CA50 steel bars. The constitutive model for these materials is described through a bilinear approximation of the stress-strain behavior, as presented in the following.

The model for the behavior of concrete was based on recommendations established by Eurocode 2 [3] and *fib* [1-2], as shown on Figure 6. The following assumptions are used to define this simplified model:

- although in some scenarios tensile stresses may play a non-negligible role in structural strength, any structural strength associated with tensile loading is not taken into account, *i.e.* concrete under tension is considered to be fully cracked and the corresponding tensile stresses are neglected;
- strains and stresses are linearly proportional on the ascending part of the curve, as recommended by Eurocode 2 [3], instead of the nonlinear curve proposed by *fib* [1-2]. Young's moduli were set as 32 GPa for C30 and 25 GPa for C20 concrete, respectively;
- for quasi-static loading conditions, the plastic regime is represented by a plateau at a stress of 37.9 MPa for C30 concrete and 20 MPa for C20 concrete;
- the ultimate strain under compression in both types of concrete is defined as 0.35%, after which any increase in the strain level will immediately decrease the stress to zero and keeps it at this level in the subsequent loading steps. In this work, this assumption associated with the multilayer discretization allows the investigation of material degradation due to compressive concrete failure (crushing).

According to Eurocode 2 [3] and NBR 6118 [4], the bilinear curve on Figure 7 represents the relationship between stress and strain for steel under quasi-static loading conditions. The following additional information can also be related to the constitutive behavior of S500 steel and CA50 steel:

- the steel behavior in tension is similar in both compression and tension;
- buckling of compressed steel bars is not considered;
- the elastic modulus, yield stress and ultimate strain are equal to 200 GPa, 500 MPa and 4%, respectively;
- just as it was assumed for concrete, stresses in the layers vanish as the strain reaches values larger than 4%, representing steel fracture;
- the ratio between ultimate stress and yield stress is equal to 1.06 (Iribarren *et al.* [16]).

In order to account for the strength enhancement provided by the strain rate dependence of both steel and concrete material behavior (Bischoff and Perry [25]; Malvar and Crawford [26]), the constitutive models defined above are extended by a strain rate dependent material behavior. The elastic modulus of concrete is therefore made dependent on the strain rate, see Iribarren *et al.* [16]) for more details. Moreover, to include the strain rate effects in the irreversible behavior of concrete and steel, a Perzyna type viscoplastic model is used (Heeres *et al.* [27]), introducing viscous terms in the constitutive laws. The viscoplastic strain rate, as used in Iribarren *et al.* [16]), is a function of the overstress value *f* and is given as follows:

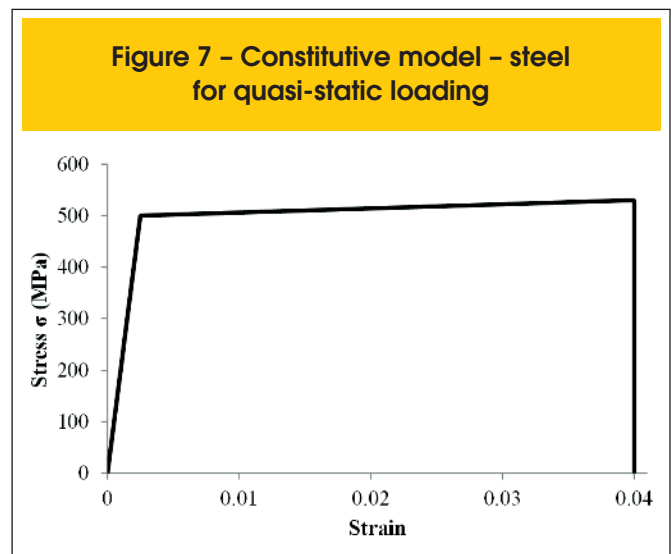
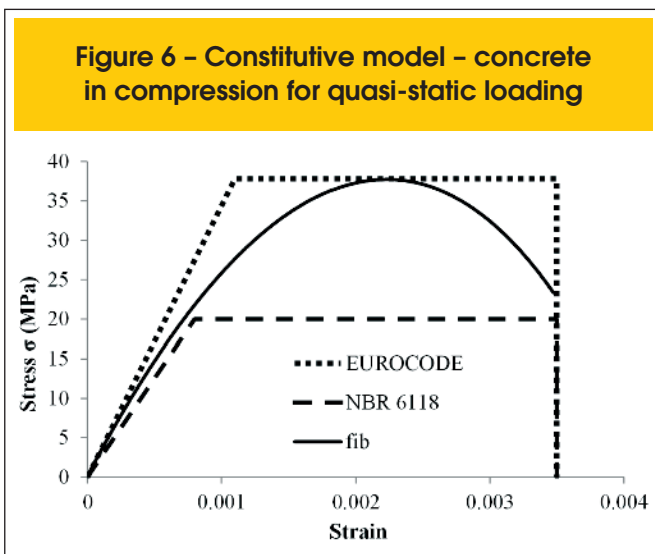
$$\dot{\epsilon}^{vp} = \frac{1}{\eta} \left\langle \frac{f}{\bar{\sigma}_0} \right\rangle^N \frac{df}{d\sigma} \tag{7}$$

where $\langle \rangle$ are called MacAulay brackets, $\dot{\epsilon}^{vp}$ is the viscoplastic strain rate, η is the initial yield stress; η and N are viscosity parameters. The parameter $\bar{\sigma}_0$ depends on the strain rate and $= 1$, as assumed by Iribarren *et al.* [16] in order to obtain a good agreement with the experimental results of Malv ar and Crawford [26]. The overstress function (*f*) is given by $(\sigma - \sigma_y)$, where σ is the one-dimensional stress and σ_y is the current yield stress.

4.4 Governing equations in dynamics

Since progressive collapse is a dynamic phenomenon, the structural equilibrium is described in a dynamic framework in the numerical model. Equilibrium in dynamics is represented by the following equation:

$$\{f_{int}(\{q\}, \{\dot{q}\})\} + [M]\{\ddot{q}\} = \{f_{ext}\} \tag{8}$$



on which an implicit Newmark integration scheme is applied and where $\{f_{int}\}$ represents the internal force vector, dependent on the displacements $\{q\}$ and the displacements rates $\{\dot{q}\}$. The mass matrix is represented by $[M]$, $\{q\}$ is the vector of nodal accelerations and $\{f_{ext}\}$, the external force vector. Note that no numerical/artificial damping is introduced in the system of equations.

Since the internal forces are strain rate dependent, their variation with respect to the displacements, *i.e.* the structural tangent operator, is also dependent on those rates and therefore introduces a

viscous damping term:

$$[K_T] = \left. \frac{\partial \{f_{int}(\{q\}, \{\dot{q}\})\}}{\partial \{q\}} \right|_{\{\dot{q}\}=cte.} + \left. \frac{\partial \{f_{int}(\{q\}, \{\dot{q}\})\}}{\partial \{\dot{q}\}} \right|_{\{q\}=cte.} \frac{\partial \{\dot{q}\}}{\partial \{q\}} \quad (9)$$

In the previous equation, the second term on the right side introduces damping at the structural level due to the strain rate dependent

Figure 8 - Deformed configuration
(displacements multiplied by 10, dashed lines relate to Figure 10)

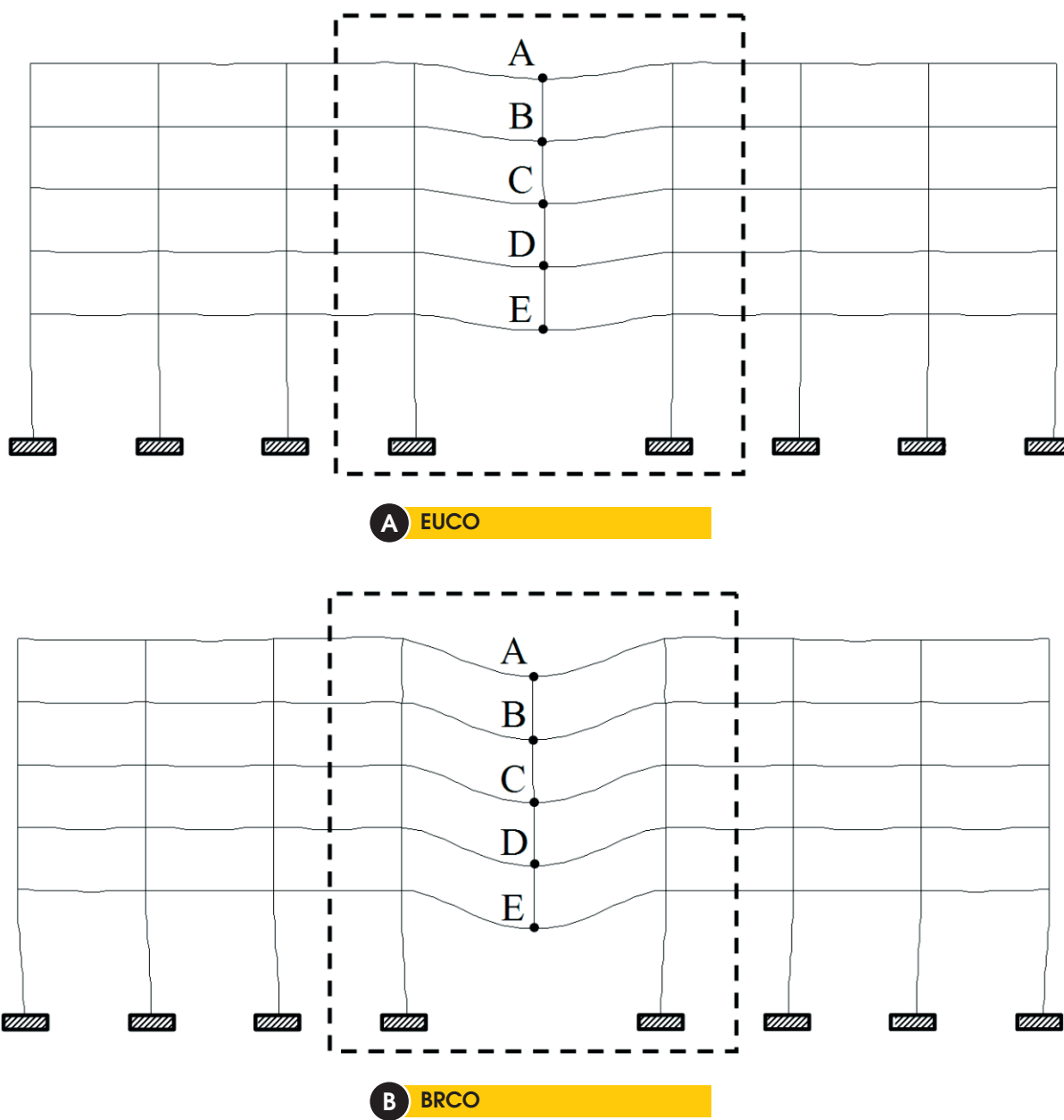
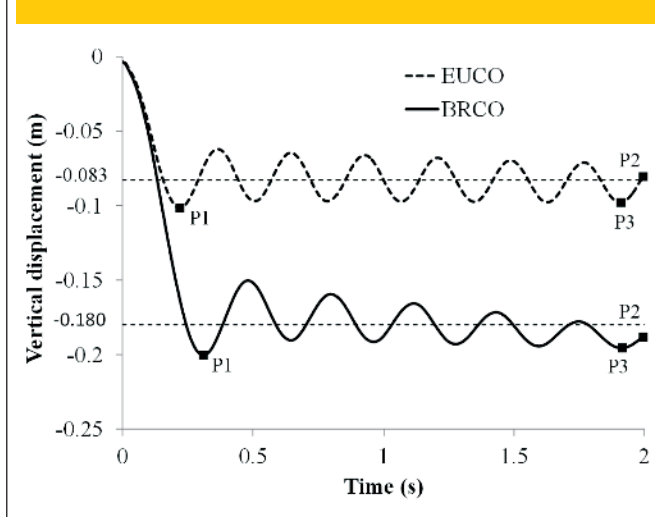


Figure 9 – Vertical displacement of point E, as a function of time



(viscoplastic) stress-strain relationships assumed for the materials. It should be noted that the mass matrix of the beam elements was here calculated considering the undeformed shape of the structure and kept constant along the entire analysis in this work. Updating the mass matrix as a function of the displacements of the structure is part of future work and can be based on Le *et al.* [28]).

The computational formulation presented in this section was carefully validated using results from the literature for steel beams and frames (Crisfield [17], Battini [18]) and also for reinforced concrete frames (Lew *et al.* [19]; Yi *et al.* [20]), which consisted on a correlation to experimental results.

5. Nonlinear dynamics simulation results

Each plane frame has the same 2D discretization, constituted from approximately 900 beam elements. Forty layers are used for the discretization of the columns cross sections and sixty layers for the

beams. The structure self-weight and service loads are applied in a large period of time, defined as 1000 s, in order to prevent the influence of dynamic effects in the initial loading phase, which is ideally quasi-static. The column removal is modeled as the decrease of the reaction forces applied at point E, equivalent to the presence of the 5th ground column (Fig. 8). This is done in a short period of time (0.01 s), subsequently to the initial loading process. The response of the structure is analyzed for a period of two seconds after column removal, as in Iribarren *et al.* [16]. The removal time corresponds to 0.5% of the response time, which classifies the loading as *impulsive* (Smith and Hetherington [29]).

The removal of a column results in the inversion of the bending moments applied on the beams which must resist these changes. Results show that the reinforcements did not fail. Consequently the structures did not collapse with the middle column removal, *i.e. both structures were able to overcome the loss of the column and did not initiate the progressive collapse mechanism, according to the simulation.* The deformed configuration of the EUCO (Eurocode-based frame) and BRCO (NBR-based frame) is shown in Figure 8. It is clearly noticeable that the displacements in BRCO are larger (Figs. 8 and 9). In fact, BRCO's vertical displacements on the reference points A-E are approximately 2 times larger than the ones of EUCO (Tab. 2). The displacement values shown on Table 2 also imply that the columns located between points A and E (Fig. 8) undergo rigid body motion.

Within the time interval defined by points P1 and P2 in Figure 9, the mean value of the displacement of point E (Fig. 8) is of approximately 8 cm and 18 cm for EUCO and BRCO analysis, respectively. Table 2 displays the vertical displacements of the reference point E for both structures. As the structures have different frequency of the displacement oscillation, the values shown on Table 2 were taken as the largest immediate displacements before the analysis completion, identified on Figure 9 by point P3.

The frequency of the displacement oscillation is slightly higher for EUCO frame. There are two explanations for the larger displacements of the Brazilian frame: 1) BRCO's structural elements have smaller sections and less reinforcement and 2) the material behavior adopted for concrete in the two simulations is different as well (Fig. 6).

The state of individual structural members at any time is available from the numerical computing. In Figure 10, the symbol (■) was used to represent sections in which steel has reached yielding and (∇) represents those in which concrete was crushed in less than 30% of the layers. It can be seen that, for both frames, the effects

Table 1 – Recommended beam loads

| EUROCODE – based design | | | |
|-------------------------|------|------|-------|
| Loads (kN/m) | Dead | Live | Total |
| Floor beams | 43.2 | 18.0 | 52.2 |
| Roof beams | 43.2 | 6.0 | 46.2 |
| NBR – based design | | | |
| Loads (kN/m) | Dead | Live | Total |
| Floor beams | 18.7 | 12.0 | 24.7 |
| Roof beams | 18.7 | 6.0 | 21.7 |

Table 2 – Vertical displacements (cm) at reference points, at times denoted by point P3 on Figure 9

| Reference point | EUCO (V1) | BRCO (V2) | V2 / V1 |
|-----------------|-----------|-----------|---------|
| A | -9.61 | -19.2 | 2.00 |
| B | -9.65 | -19.3 | 2.00 |
| C | -9.71 | -19.4 | 2.00 |
| D | -9.76 | -19.5 | 2.00 |
| E | -9.79 | -19.6 | 2.00 |

of the middle column removal can barely be identified on other beams and columns than the ones above the point E. However, BRCO presents a larger number of plastified sections (158 sections from BRCO against 94 sections from EUCO, Fig. 10). Differently from EUCO, BRCO also displays sections on which concrete was crushed.

According to the *Allowable Collapse Region* criterion (DoD [5]), only the bays immediately adjacent to the removed element must be affected. This indicates that only bays 4 and 5 could be affected in terms of collapse. Figure 10 shows that there was no collapse and that plastification of the steel rebars only occurs in bays 4 and 5. Therefore, the *Allowable Collapse Region* criterion was fulfilled.

6. Discussion

Both frames were designed in accordance to current building codes and consider the presence of stirrups. In this work however, stirrups are not incorporated during the PC analyses which means that their positive influence in preventing concrete cracking, if any, is neglected. The presence of stirrups could be included in the numerical model by changing the constitutive behavior of concrete, *i.e.* modifying the maximum compressive stress and the ultimate strain in order to account for the confinement of the material.

Designing the frames in accordance with two different codes, Eurocode 2 [3] and NBR 6118 [4], also resulted in using different constitutive behaviors for concrete. As seen in Figure 7, BRCO considers lower compressive strength of concrete. Using concrete with higher compressive strength for the BRCO frame may however not systematically lead to an increase in the overall robustness of the structure. This would also result in different cross sections for the

structural elements and different reinforcement schemes during the structural design step. Therefore a new set of PC simulations should be conducted to assess the influence of such a variation.

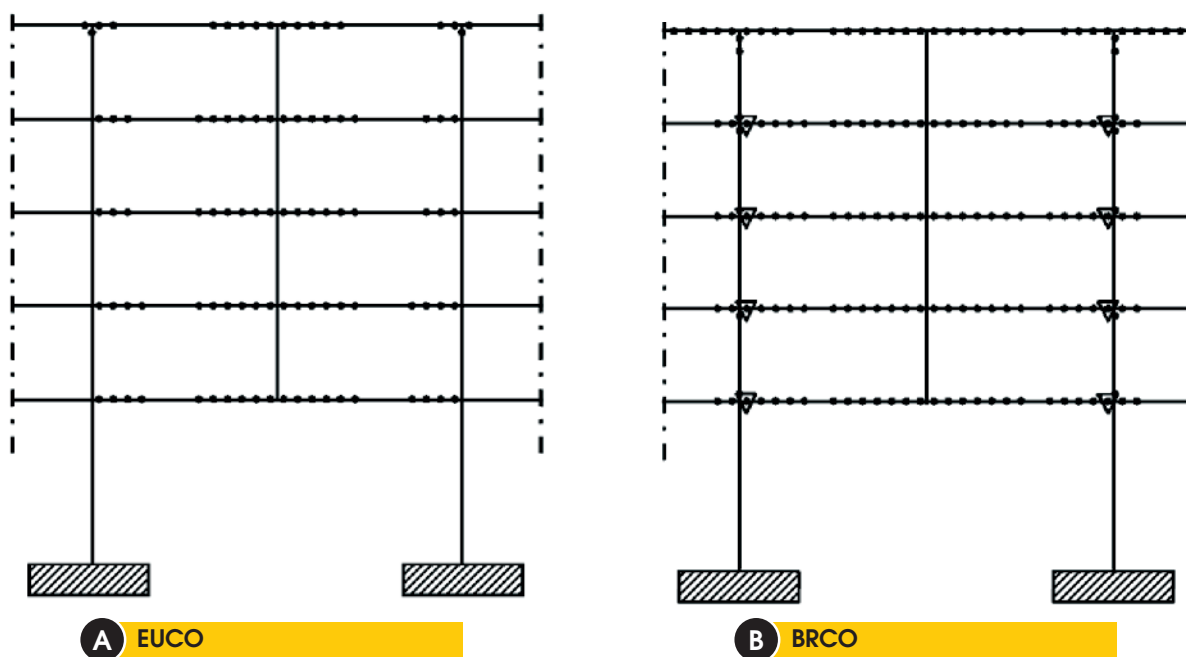
Given the multiscale approach of the PC problem discussed here, it was necessary to define an optimum number of layers for discretizing the members cross sections, *i.e.* not too many layers that would make the analysis unaffordable in terms of computational time or too few that would introduce significant errors in the results obtained. A preliminary step to establish the minimum number of layers to be used for the element cross sections is suggested for every new design.

The oscillation of the point above the removed column is of high importance, since it implies repeated cyclic variations of the structural stress level. This scenario may accelerate the process of concrete crushing and introduce material damage.

Both designs were able to resist PC, and the plastic strain distribution was localized in the two bays above the removed column. This type of localized damage is of restricted extent which may decrease the number of losses and result in easier repair of the remaining structure. Nevertheless, it is important to stress that the plasticity distribution and structural damage may be strongly dependant on the position of the removed column (Iribarren *et al.* [16]), and a more wide-spread damage may be expected in other scenarios.

Additional analyses using a geometrically linear formulation showed a response similar to the one described earlier. This implies that the positive influence of (geometrically nonlinear) catenary effects in mitigating PC could not be triggered in the considered simulations due to the relatively small displacements in the structure. However, this point should be further investigated in future works in 3D simulations and also in the analyses of different

Figure 10 - Plasticity distribution on the undeformed configuration, at the end of the analysis (2s after middle column removal; for the sake of good visibility, only the affected areas were represented)



RC frames.

As buildings are spatial structures, analyzing PC via a bidimensional formulation inevitably carries limitations. At a higher computational cost, a tridimensional approach would allow the inclusion of shear and torsional effects and would also permit the modeling of failure along the three axes, allowing a more complete understanding of the phenomenon.

For this work, the complete multiscale PC analysis of one structure took approximately 8 hours on an Intel i5 3.0 GHz personal computer, using a single CPU core for the computation. The computational performance could be significantly enhanced using a parallel computation scheme, which is part of future work.

Energy conservation problems associated to the use of the corotational formulation in the solution of nonlinear dynamic problems were reported by Crisfield and Shi [30] and Salomom *et al.* [31]. This inconvenience is shown to be related to the adopted time step and tends to be more severe the latter gets larger. In this work, however, time steps were in the order of 0.01s and the occurrence of such problems was not verified.

7. Concluding remarks

This work presented the computational analysis of two reinforced concrete plane frames designed in accordance with the minimum requirements of two different building codes, from Europe and from Brazil. The problem is approached taking into account dynamic effects, as well as material and geometrical nonlinearities. A multilayered Bernoulli beam element using corotational kinematics was developed for this purpose. The details and assumptions made during the design process were provided, as well as a summary of the applied numerical formulation and the material constitutive behavior.

None of the structures triggered the progressive collapse mechanism after the removal of a middle column, which implies that the minimum requirements of both codes are successful in providing structural robustness for the particular scenarios studied here. Larger displacements were observed for the Brazilian frame as a result of weaker design constraints. For both frames, the structural damage happened to be localized only on the floors immediately above the removed middle column.

Future research includes the updating of the structure mass matrix as a function of structural deformation, the association of plasticity and damage (elastic stiffness degradation) in the representation of the constitutive material behavior, and the use of a formulation including shear effects. The ultimate goal is the extension of the formulation to three dimensional structures which will require a parallel implementation of the code and would allow for the inclusion of the resistance introduced by the concrete slabs and also by the out-of-plane beams.

8. Acknowledgments

The authors would like to thank CAPES, CNPq, FAPEMIG, Fundação Gorceix and PROPEC for the financial support. The third author was sponsored by the Fonds de la Recherche Scientifique F.R.S. - FNRS of Belgium (post-doctoral research grant 'Chargé de Recherches' N^o. 1.2.093.10.F). The authors also acknowledge the support of F.R.S. - FNRS Belgium (grant N^o. 1.5.032.09.F) for the

intensive computational facilities used for this work.

9. References

- [01] INTERNATIONAL FEDERATION FOR STRUCTURAL CONCRETE (fib), Constitutive modelling of high strength/high performance concrete, State-of-art report, fib Bulletin 42, 2008a.
- [02] INTERNATIONAL FEDERATION FOR STRUCTURAL CONCRETE (fib), Practitioners' guide to finite element modelling of reinforced concrete structures. State-of-art report, fib Bulletin 45, 2008b.
- [03] EUROCODE 2: Design of concrete structures - Part 1-1: General rules and rules for buildings, December, 2004.
- [04] NBR 6118: projeto de estruturas de concreto: procedimento, ABNT - Associação Brasileira de Normas Técnicas, Rio de Janeiro, 2003.
- [05] DEPARTMENT OF DEFENSE (DOD), Unified Facilities Criteria (UFC): Design of buildings to resist progressive collapse, UFC 4-023-03, Washington DC, 2009.
- [06] LI, Y., LU, X., GUAN, H., YE, L., An improved tie force method for progressive collapse resistance design of reinforced concrete frame structures, *Engineering Structures*, Vol. 33, 2931–2942, 2011.
- [07] KIM, H.-S., KIM, J., AN, D.-W., Development of integrated system for progressive collapse analysis of building structures considering dynamic effects, *Advances in Engineering Softwares*, Vol. 40, 1–8, 2009.
- [08] TSAI, M.-H., LIN, B.-H., Investigation of progressive collapse resistance and inelastic response for an earthquake-resistant RC building subjected to column failure, *Engineering Structures*, Vol. 30, 3619–28, 2008.
- [09] KWASNIEWSKI, L., Nonlinear dynamic simulations of progressive collapse for a multistore building, *Engineering Structures*, Vol. 32, 1223–35, 2010.
- [10] TAN, K. H., PHAM, X. D., Membrane actions of RC slabs in mitigating progressive collapse of building structures. *Proceedings of the Design and Analysis of Protective Structures*, Singapore, 2010.
- [11] MARJANISHVILI, S. M., Progressive analysis procedure for progressive collapse, *Journal of Performance of Constructed Facilities*, Vol. 18(2), 79–85, 2004.
- [12] IZZUDDIN, B. A., Robustness by design – Simplified progressive collapse assessment of building structures, *Stahlbau*, Vol. 79, 556–564, 2010.
- [13] KHANDELWAL K., EL-TAWIL S., Pushdown resistance as a measure of robustness in progressive collapse analysis, *Engineering Structures*, Vol. 33, 2653–2661, 2011.
- [14] BUILDSOFT NV, Diamonds 2010 r.01, <http://www.buildsoft.eu> (Last access: 07/02/2014).
- [15] CYPE, Cypecad 2011, <http://www.cype.pt> (Last access: 07/02/2014).
- [16] IRIBARREN, B. S., BERKE, P., BOUILLARD, PH., VAN-TOMME, J., MASSART, T. J., Investigation of the influence of design and material parameters in the progressive collapse analysis of RC structures, *Engineering Structures*, Vol. 33, 2805–2820, 2011.
- [17] CRISFIELD, M. A., *Non-Linear Finite Element Analysis of Solids and Structures*, Vol. I. John Wiley & Sons, 1997.
- [18] BATTINI, J.-M., Corotational beam elements in instability problems, Ph.D Thesis, Royal Institute of Technology, De-

- partment of Mechanics, Stockholm, Sweden, 2002.
- [19] LEW, H. S., BAO, Y., SADEK, F., MAIN, J. A., PUJOL, S., & SOZEN, M. A., An Experimental and Computational Study of Reinforced Concrete Assemblies under a Column Removal Scenario, NIST Technical Note 1720, U.S. Department of Commerce, 2011.
- [20] YI, W.J., HE, Q.F., XIAO, Y., AND KUNNATH, S. K., Experimental Study on Progressive Collapse-Resistant Behavior of Reinforced Concrete Frame Structures, *ACI Structural Journal*, Vol. 105:4, 433-440, 2008.
- [21] LEE, Y. H., SCANLON, A., Comparison of One- and Two-Way Slab Minimum Thickness Provisions in Building Codes and Standards, *ACI Structural Journal* Vol. 107:2, 157-163, 2010-3.
- [22] BONET, J. WOOD, R. D., *Nonlinear continuum mechanics for finite element analysis*, Cambridge University Press, 1997.
- [23] BATTINI, J.-M., NGUYEN, Q.-H., HJIAJ, M., Non-linear finite element analysis of composite beams with interlayer slips, *Computer and Structures*, Vol. 87, 904-912, 2009.
- [24] SOUSA JR., J. B. M., OLIVEIRA, C. E. M., SILVA A. R., Displacement-based nonlinear finite element analysis of composite beam columns with partial interaction, *Journal of Constructional Steel Research*, Vol. 66, 772 -779, 2010.
- [25] BISCHOFF, P. H, PERRY, S. H., Compressive behavior of concrete at high strain rates, *Materials and Structures*, Vol. 24, 425-50, 1991.
- [26] MALVAR, L. J, CRAWFORD, J. E., Dynamic increase factors for concrete, 28th DDESB seminar, Orlando, FL, USA, 1998.
- [27] HEERES O. M., SUIKER A. S. J., DE BORST R., A comparison between the Perzyna viscoplastic model and the consistency viscoplastic model, *European Journal of Mechanics A/ Solids*, Vol. 21, 1-12, 2002.
- [28] LE, T.-N., BATTINI, J.-M., HJIAJ, M., Efficient formulation for dynamics of corotational 2D beams, *Computational Mechanics*, Vol. 48, 153-161, 2011.
- [29] SMITH P. D., HETHERINGTON J. G., *Blast and ballistic loading of structures*, Butterworth Heinemann, London, 1994.
- [30] CRISFIELD, M. A., SHI, J., An energy conserving co-rotational procedure for non-linear dynamics with finite elements, *Nonlinear Dynamics*, Vol.9, 37-52, 1996.
- [31] SALOMON, J., WEISS, A. A., WOHLMUTH, B. I., Energy-conserving algorithms for a corotational formulation, *SIAM Journal on Numerical Analysis*, Vol. 46, 1842-1866, 2008.